Heat Conduction in the Vortex State of $NbSe_2$: Evidence for Multiband Superconductivity

Etienne Boaknin,[1] M. A. Tanatar,[1] Johnpierre Paglione,[1] D. Hawthorn,[1] F. Ronning,[1] R.W. Hill,[1] M. Sutherland,[1] Louis Taillefer,[1,2] Jeff Sonier,[2,3] S. M. Hayden,[4] and J.W. Brill[5]

[1]*Department of Physics, University of Toronto, Toronto, Ontario, Canada*
[2]*Canadian Institute for Advanced Research, Toronto, Ontario, Canada*
[3]*Department of Physics, Simon Fraser University, Burnaby, Canada*
[4]*H. H. Wills Physics Laboratory, University of Bristol, Bristol BS8 1TL, United Kingdom*
[5]*Department of Physics and Astronomy, University of Kentucky, Lexington, Kentucky, 40506-0055*
(Received 15 November 2002; published 18 March 2003)

The thermal conductivity κ of the layered s-wave superconductor $NbSe_2$ was measured down to $T_c/100$ throughout the vortex state. With increasing field, we identify two regimes: one with localized states at fields very near H_{c1} and one with highly delocalized quasiparticle excitations at higher fields. The two associated length scales are naturally explained as multiband superconductivity, with distinct small and large superconducting gaps on different sheets of the Fermi surface. This behavior is compared to that of the multiband superconductor MgB_2 and the conventional superconductor V_3Si.

DOI: 10.1103/PhysRevLett.90.117003 PACS numbers: 74.70.Ad, 74.25.Fy, 74.25.Jb, 74.25.Qt

Multiband superconductivity (MBSC) is the existence of a superconducting gap of significantly different magnitude on distinct parts (sheets) of the Fermi surface (FS). This unusual phenomenon has recently emerged as a possible explanation for the anomalous properties of some s-wave superconductors. Although first experimentally observed over 20 years ago [1], the possible existence of MBSC has not often been considered since then. The current interest in MBSC has been fueled by the peculiar properties of the 40-K superconductor MgB_2, where the case for MBSC is now rather compelling [2]. In particular, a gap much smaller than the expected BCS gap has been resolved in tunneling experiments [3]. One consequence of a small gap is the ability to easily excite quasiparticles, which, for example, can make the properties of this s-wave superconductor similar to those of d-wave superconductors.

Based on angle-resolved photoemission (ARPES) measurements, it has recently been proposed that the 7-K layered superconductor $NbSe_2$ is also host to MBSC [4]. A sizable difference in the magnitude of the superconducting gap was found on two sets of Fermi surface sheets, with no detectable gap on the smallest sheet. However, these measurements were performed only at 5.3 K. It is clearly of interest to shed further light on this sheet-dependent superconductivity by performing bulk measurements down to low temperatures.

In this Letter, we report a study of heat transport in $NbSe_2$ down to $T_c/100$ throughout the vortex state, providing further evidence for MBSC. By measuring the degree of delocalization of quasiparticle states in the vortex state, heat transport probes the overlap between core states on adjacent vortices, i.e., the size of the vortex core ($\sim \xi$), and hence the magnitude of the gap ($\sim 1/\xi$). We resolve two regimes of behavior: one limited to very low fields (up to $\sim 5H_{c1}$), where delocalization is slow and activated as in conventional (single-gap) superconductors such as V_3Si, and one for all other fields up to H_{c2} where quasiparticles transport heat extremely well, as in unconventional superconductors with nodes in the gap.

$NbSe_2$, a quasi-2D metal with hexagonal symmetry, displays a transition to a charge density wave state around $T \simeq 35$ K. Measurements of its FS at low temperatures, by both de Haas–van Alphen (dHvA) [5] and ARPES measurements [4], agree with band structure calculations that predict a FS made of four or five sheets. These sheets divide into two groups: a small Γ-centered pocket derived from the Se $4p$ band (denoted as Γ band) and larger nearly two-dimensional sheets derived from Nb $4d$ bands. Scanning tunneling spectroscopy (STS) at 50 mK revealed a spectrum that is consistent with a distribution of gaps that range from 0.7 to 1.4 meV [6]. In the vortex state at very low fields (near H_{c1}), a zero-bias conductance peak, characteristic of states localized in the vortex core, was observed at the vortex center [7].

The thermal conductivity κ of $NbSe_2$ was measured in a dilution refrigerator using a standard technique [8]. Measurements were made at temperatures increasing from 50 mK and in magnetic fields ranging from 0 to 6 T, applied parallel to the c axis and perpendicular to the in-plane heat current. The sample was cooled in field to ensure field homogeneity. Measurements as a function of field at fixed temperature resulted in nearly no difference as compared to the field-cooled data [see Fig. 2(a)].

The sample, a rectangular parallelepiped with dimensions 1.2×0.5 mm in the plane and 0.1 mm along the c axis, is from the same batch as the sample used by Sonier *et al.* [10,11] and has a superconducting transition temperature $T_c = 7.0$ K with a width $\delta T_c = 0.1$ K. It was cleaved to provide six fresh surfaces for silver paint contacts with resistances at low temperatures of roughly 20 mΩ. The residual resistivity ratio is 40 ($\rho_0 \simeq$

$3\ \mu\Omega\,\mathrm{cm}$), and the upper and lower critical fields are, respectively, $H_{c2} = 4.5$ T and $H_{c1} = 20$ mT for $H \parallel c$. The coherence length estimated from H_{c2} is $\xi(0) = 85$ Å.

The thermal conductivity of $NbSe_2$ is plotted in Fig. 1, as κ/T against T^2. This enables a separation of the electronic and the phononic thermal conductivities, since the asymptotic T dependence of the former as $T \to 0$ is linear while that of the latter is cubic. The electronic thermal conductivity κ_0/T is thus obtained as the extrapolated $T \to 0$ value. In zero field, $\kappa_0/\mathrm{T} = 0.000 \pm 0.005\ \mathrm{mW\,K^{-2}\,cm^{-1}}$, a clear indication that $NbSe_2$ is an s-wave superconductor with a fully gapped excitation spectrum. However, by applying a small magnetic field ($H \geq H_{c1}$), an electronic contribution develops as a rigid shift from the $H = 0$ curve in Fig. 1. At higher fields ($H \geq 1.5$ T), the electronic contribution dominates the conduction over the entire temperature range and κ/T is constant in temperature within our experimental resolution. Above H_{c2}, the Wiedemann-Franz (WF) law is satisfied and the thermal conductivity saturates.

The κ_0/T values are plotted as a function of H on a reduced scale in Fig. 2. Also plotted is a field sweep at $T = 130$ mK from which the zero-field value (the phononic contribution) has been subtracted. As seen in Fig. 2(c), heat conduction starts to increase right at H_{c1} in what could be qualified as an activated behavior, although in a very limited range of fields: $H_{c1} \leq H \leq 0.03H_{c2}$. (The value of H_{c1} is determined *in situ* as the drop in the phonon κ due to vortex scattering.) At higher fields, κ_0/T increases rapidly, i.e., faster than $(H/H_{c2})\ \kappa_N/T$, where κ_N/T is the normal state value. This shows the presence of *highly delocalized quasiparticle states almost throughout the vortex state of* $NbSe_2$.

This is in stark contrast to the behavior expected of a type-II s-wave superconductor. Indeed, when a field in excess of H_{c1} is applied, and vortices enter the sample, the conventional picture is that the induced electronic states are *localized* within the vortex cores. As one increases the field, the intervortex spacing $d \simeq \sqrt{\Phi_0/B}$ decreases. The localized states in adjacent vortices will have an increasing overlap leading to enhanced tunneling between vortices and the formation of conduction bands. Strictly speaking, the electronic states are actually

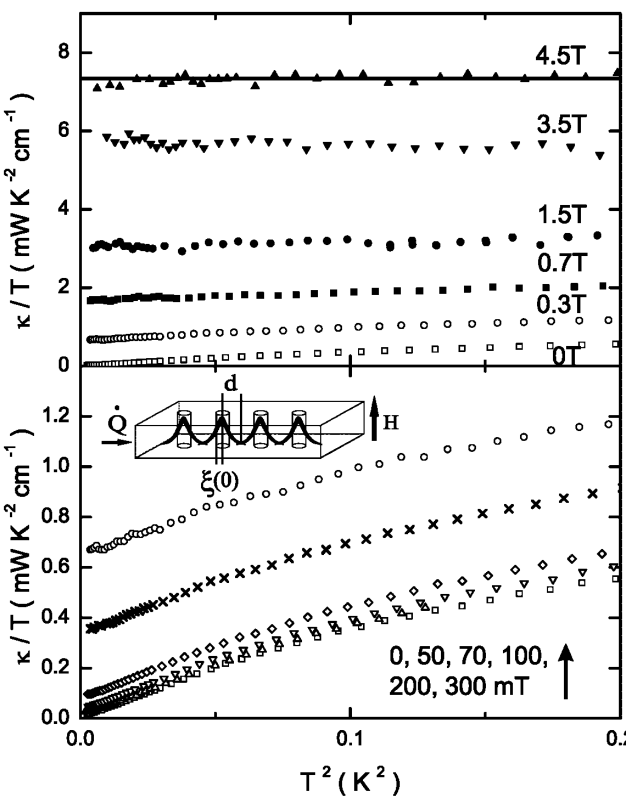

FIG. 1. Thermal conductivity of $NbSe_2$ at several applied fields, plotted as κ/T vs T^2. The solid line indicates the value expected from the Wiedemann-Franz law as obtained from resistivity measurements at $H = 4.5$ T. The field is applied parallel to the c axis and perpendicular to the heat current $\dot{Q}$.

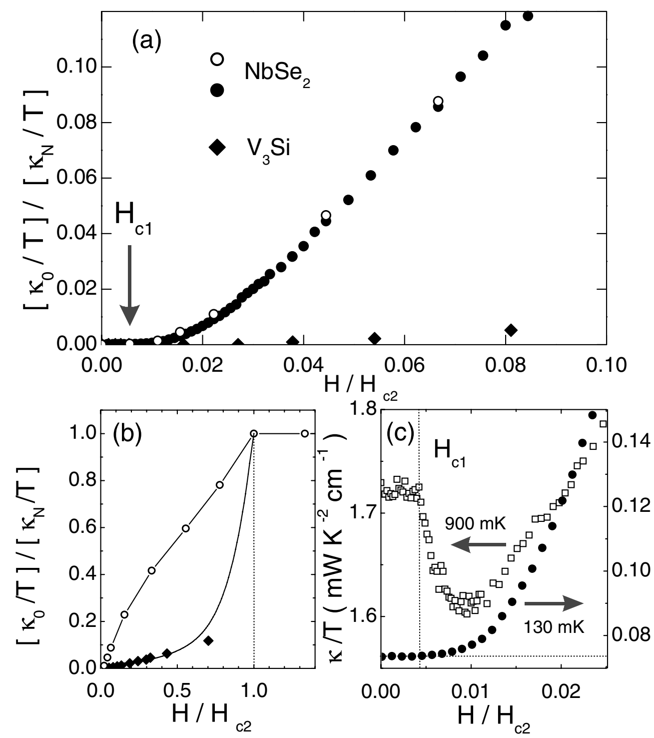

FIG. 2. (a),(b) Thermal conductivity of $NbSe_2$ (empty circles) and V_3Si (diamonds) at $T \to 0$ vs H, normalized to values at H_{c2}. Filled circles come from a sweep in field at $T = 130$ mK from which the $H = 0$ thermal conductivity (phononic contribution) has been subtracted. The thick solid line in (b) is a theoretical curve for the thermal conductivity of V_3Si [9]. The thin line is a guide to the eye. (c) κ/T vs H for $NbSe_2$ at $T = 130$ mK (circles) and $T = 900$ mK (squares). The latter shows a typical drop in the phononic thermal conductivity at $H_{c1} = 20$ mT. The former shows that the electronic thermal conductivity starts to increase right at H_{c1} but has a slow activated-like behavior for fields below $0.03H_{c2}$.

always delocalized but with extremely flat bands at low fields [12]. As these gradually become more dispersive, the thermal conductivity should increase accordingly and grow exponentially with the ratio d/ξ, as is indeed observed in Nb [13].

A better point of comparison for $NbSe_2$ is V_3Si, an extreme type-II superconductor with comparable superconducting parameters ($T_c = 17$ K, $\xi = 50$ Å). This is done in Fig. 2, where the thermal conductivity of V_3Si is seen to grow much more slowly with H than that of $NbSe_2$, as described by theory [9]. Quantitatively, at $H = H_{c2}/20$, $\kappa_0/T = \frac{1}{20} \times \kappa_N/T$ for $NbSe_2$ and $\frac{1}{400} \times \kappa_N/T$ for V_3Si [14]. Note that the samples compared in Fig. 2 are in the same regime of purity. From the standard relation $\xi(0) = 0.74\xi_0[\chi(0.88\xi_0/l)]^{1/2}$, we obtain for V_3Si $\xi_0/l = 0.13$, with $\xi(0) = 50$ Å from H_{c2} and $l = 1500$ Å from dHvA [15]. This is similar to the value of 0.15 for $NbSe_2$ [16].

The high level of delocalization in $NbSe_2$ is a clear indication of either a gap with nodes (e.g., d wave) or a nodeless gap which is either highly anisotropic or small on one FS and large on another. A gap with nodes is ruled out by the absence of a residual term in the thermal conductivity in zero field [17].

It is revealing to compare $NbSe_2$ to MgB_2, for which the thermal conductivity has a similar field dependence. Strikingly, κ follows roughly the same field dependence as the specific heat C for both $NbSe_2$ and MgB_2. This is shown in Fig. 3 where $\kappa(H)$ and $C(H)$ are plotted on a reduced field scale for single crystals of $NbSe_2$ [10,18], MgB_2 [19,20], and V_3Si [21,22], with $H \parallel c$ for hexagonal $NbSe_2$ and MgB_2, and $H \parallel a$ for cubic V_3Si. In conventional superconductors such as V_3Si, $\kappa(H)$ and $C(H)$ are very different [see Fig. 3(c)] because the excited electronic states are largely localized.

MgB_2 is a well-established case of MBSC with a small gap on one FS ($\Delta_\pi = 1.8$ meV) and a large gap on the other ($\Delta_\sigma = 6.8$ meV). The field dependence of its heat capacity is well understood in this context [20], with a distinctive shoulder at a field of $H_{c2}/10$ [see Fig. 3(b)] [23]. A similar shoulder is also manifest in $NbSe_2$ around $H_{c2}/9$ [see Fig. 3(a)]. Empirically, the striking fact that heat transport and heat capacity have the same field dependence in both materials points to a common explanation and hence suggests that *$NbSe_2$ is host to multiband superconductivity* [24]. This is consistent with recent ARPES measurements at $T = 0.8T_c$ [4].

In conventional superconductors, the delocalization of vortex core bound states occurs gradually on the scale of H_{c2}, and the characteristic length scale is $\xi(0) \simeq \sqrt{\Phi_0/2\pi H_{c2}}$. It appears that in $NbSe_2$ (and MgB_2), there are two characteristic length scales for delocalization: ξ^* and $\xi(0)$. To see this, we focus on the low-field region. For $NbSe_2$, both κ/T and C/T have been measured with high precision on the same crystals, thereby making a detailed comparison possible. Figure 4(a) shows the comparison for fields below $H_{c2}/10$, where the two do not coincide: C/T increases abruptly above H_{c1} while κ/T grows slowly, in an activated way. This is consistent with the presence of localized states at very low fields as imaged by STS [6,7]. Then this behavior gives way to a rapid increase of the thermal conductivity at fields above $0.03H_{c2}$. This is a clear indication that the field scale associated with delocalization in $NbSe_2$ is much smaller than H_{c2}.

In fact, we can scale the behavior of the low-field thermal conductivity of $NbSe_2$ to that of V_3Si using $H^* = H_{c2}/9$ [Fig. 4(b)]. This is also seen clearly if we plot the ratio of the thermal conductivity to the specific heat [Fig. 4(c)] which measures the degree of delocalization. The ratio is seen to have two regimes: a rapid increase below $H^* \simeq H_{c2}/10$ and a slow one above. In summary, the second length scale associated with delocalization in $NbSe_2$ is $\xi^* \simeq \xi(0)/\sqrt{9} = \xi(0)/3$. This is consistent and

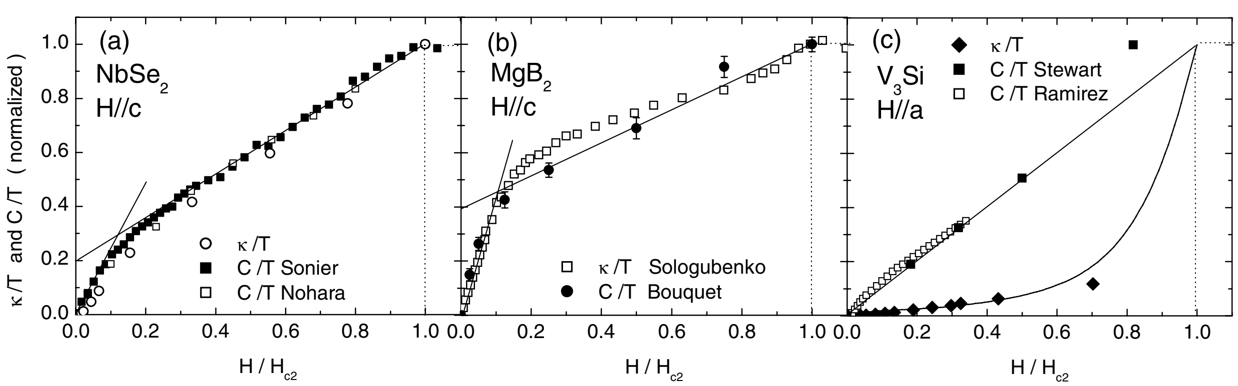

FIG. 3. (a) Thermal conductivity and heat capacity of $NbSe_2$ normalized to the normal state value vs H/H_{c2}. The heat capacity was measured in two different ways: (i) at $T = 2.4$ K on the same crystals as used in this study [10], and (ii) extrapolated to $T \rightarrow 0$ from various temperature sweeps on different crystals [18]. (b) Equivalent data for MgB_2 single crystals [19,20]. (c) Equivalent data for V_3Si, with a theoretical curve for κ/T [9]. The specific heat is measured at $T = 3.5$ K [21] and extrapolated to $T = 0$ [22]. The straight line is a linear fit. The thermal conductivity is seen to follow the specific heat very closely for both $NbSe_2$ and the multiband superconductor MgB_2. It does not, however, for the conventional s-wave superconductor V_3Si.

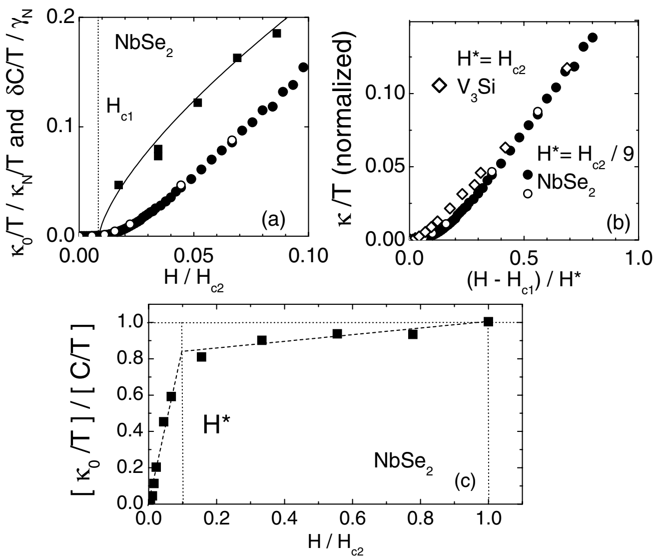

FIG. 4. (a) Thermal conductivity (circles) and the field evolution of the heat capacity $\delta C/T = [C(T,H) - C(T,H=0)]/T$ (squares) [10] of $NbSe_2$ normalized to the normal state values vs H/H_{c2} at very low fields. The line is a guide to the eye. (b) Normalized thermal conductivity vs $(H - H_{c1})/H^*$ for $NbSe_2$ and V_3Si with $H^* = H_{c2}/9$ and H_{c2}, respectively. (c) Ratio of heat transport to heat capacity in $NbSe_2$.

may explain naturally the shrinking of the vortex cores observed with muon spin rotation [11].

Considering the fact that the upper critical field is related to the superconducting gap by $H_{c2} \propto \Delta^2/v_F^2$ where v_F is the Fermi velocity, we estimate the gap to vary over the FS by a factor of 3 ($\Delta^* \simeq \Delta_0/3$). (Note that we assume v_F to be constant, within the direction of the *ab* plane, as found by band structure calculations [5].) A variation of this order was reported earlier from STS measurements [6], where the spread in Δ was measured to be between 0.7 and 1.4 meV. Moreover, theoretical modeling of STS features associated with the vortex cores [25] and efforts to model $C(T)$ [26] were found to require an anisotropy in the gap of a factor of 3 and 2.5, respectively.

Our results are consistent with dHvA measurements [15]: while extended quasiparticles are seen deep into the vortex state in both $NbSe_2$ and V_3Si, the additional damping attributed to the superconducting gap below H_{c2} increases more slowly in $NbSe_2$. Corcoran *et al.* measured the electron-phonon constant $\lambda_{\text{e-ph}} = 0.3$ for the Γ band whereas they extract an average value of $\lambda_{\text{e-ph}} = 1.8$ from specific heat [5]. The origin of MBSC may lie in the fact that $\lambda_{\text{e-ph}}$ is smaller for the Γ band. This suggests that superconductivity originates in the Nb $4d$ bands and is induced onto the Se $4p$ Γ pocket.

In summary, measurements of heat transport in the vortex state of $NbSe_2$ at low temperatures reveal the existence of highly delocalized quasiparticles down to fields close to H_{c1}. This is in striking contrast with what is expected in a *s*-wave superconductor where well-separated vortices should support only localized states, as is observed in V_3Si. We identify two characteristic length scales that govern the destruction of superconductivity in $NbSe_2$: the usual one associated with H_{c2} and another associated with a much smaller field $H^* \simeq H_{c2}/9$. We attribute this to multiband superconductivity, whereby the gap on the pocketlike Γ band is approximately 3 times smaller than the gap on the other two Fermi surfaces.

We are grateful to H.-Y. Kee, Y. B. Kim, W. A. MacFarlane, K. Machida, A. G. Lebed, and K. B. Shamokhin for stimulating discussions. We thank Saša Dukan for providing us with theoretical calculations. This work was supported by the Canadian Institute for Advanced Research and funded by NSERC of Canada.

[1] G. Binnig *et al.*, Phys. Rev. Lett. **45**, 1352 (1980).
[2] H. J. Choi *et al.*, Nature (London) **418**, 758 (2002), and references therein.
[3] G. Rubio-Bollinger *et al.*, Phys. Rev. Lett. **86**, 5582 (2001); M. R. Eskildsen *et al.*, Phys. Rev. Lett. **89**, 187003 (2002).
[4] T. Yokoya *et al.*, Science **294**, 2518 (2001).
[5] R. Corcoran *et al.*, J. Phys. Condens. Matter **6**, 4479 (1994).
[6] H. F. Hess *et al.*, Physica (Amsterdam) **169B**, 422 (1991).
[7] H. F. Hess *et al.*, Phys. Rev. Lett. **62**, 214 (1989).
[8] E. Boaknin *et al.*, Phys. Rev. Lett. **87**, 237001 (2001).
[9] S. Dukan *et al.*, Phys. Rev. B **66**, 014517 (2002).
[10] J. Sonier *et al.*, Phys. Rev. Lett. **82**, 4914 (1999).
[11] J. Sonier *et al.*, Phys. Rev. Lett. **79**, 1742 (1997).
[12] K. Yasui and T. Kita, Phys. Rev. Lett. **83**, 4168 (1999).
[13] W. F. Vinen *et al.*, Physica (Amsterdam) **55A**, 94 (1971).
[14] For V_3Si, κ_N/T is taken to be L_0/ρ_0, from the WF law where $L_0 = \pi^2 k_B^2/3e^2$ and ρ_0 is extrapolated from the resistivity. We use $H_{c2}(0) = 18.5$ T [15].
[15] T. J. B. M. Janssen *et al.*, Phys. Rev. B **57**, 11 698 (1998).
[16] K. Takita and K. Masuda, J. Low Temp. Phys. **58**, 127 (1985).
[17] M. J. Graf *et al.*, Phys. Rev. B **53**, 15 147 (1996).
[18] M. Nohara *et al.*, J. Phys. Soc. Jpn. **68**, 1078 (1999).
[19] A. V. Sologubenko *et al.*, Phys. Rev. B **66**, 014504 (2002).
[20] F. Bouquet *et al.*, Phys. Rev. Lett. **89**, 257001 (2002).
[21] A. P. Ramirez, Phys. Lett. A **211**, 59 (1996).
[22] G. R. Stewart and B. L. Brandt, Phys. Rev. B **29**, 3908 (1984).
[23] A similar shoulder was observed in Sr_2RuO_4, S. NishiZaki *et al.*, J. Phys. Soc. Jpn. **69**, 572 (2000), possibly host to *unconventional* MBSC, D. F. Agterberg *et al.*, Phys. Rev. Lett. **78**, 3374 (1997).
[24] For a calculation that would lead to a different conclusion, see H. Kusunose *et al.*, Phys. Rev. B **66**, 214503 (2002).
[25] N. Hayashi *et al.*, Phys. Rev. Lett. **77**, 4074 (1996).
[26] D. Sanchez *et al.*, Physica (Amsterdam) **204B**, 167 (1995).